Materials Science Forum
ISSN: 1662-9752, Vol. 1062, pp 514-518
doi:10.4028/p-cxd7z3

Submitted: 2021-10-15
Revised: 2022-03-17
Accepted: 2022-03-17
Online: 2022-05-31

A Study of 4H-SiC Semi-Superjunction Rectifiers for Practical Realisation

G.W.C. Baker[1,a*], Fan Li[1,b], Tianxiang Dai[1,c], Arne Renz[1,d], Luyang Zhang[1,e], Yunyi Qi[1,f], Vishal Shah[1,g], Phillip Mawby[1,h], Marina Antoniou[1,i], Peter Gammon[1,g]

[1]University of Warwick, Coventry, United Kingdom

[a]guy.baker@warwick.ac.uk, [b]f.li.3@warwick.ac.uk, [c]Tianxiang.Dai@warwick.ac.uk, [d]A.Renz@warwick.ac.uk, [e]luyang.zhang.1@warwick.ac.uk, [f]y.qi.1@warwick.ac.uk, [g]vishal.shah@warwick.ac.uk, [h]p.a.mawby@warwick.ac.uk, [i]ma308@cam.ac.uk, [g]P.M.Gammon@Warwick.ac.uk

Keywords: superjunction, semi-superjunction, Schottky barrier diode, simulation

Abstract. This paper discusses the design and simulation of 4H-SiC semi-SJ structures producing results t

hat are below the unipolar limit, whilst also ensuring practical and cost-effective realisation. The results demonstrate that a semi-SJ structure with a 10° sidewall angle increases the implantation window of the device by 45 %, relative to the full-SJ, whilst maintaining a high V_{BD} of ~2 kV and a low $R_{ON,SP}$. This design facilitates a wide implantation window with a reduced trench aspect ratio, significantly improving the practical realisation of the device. It also offers softer reverse recovery characteristics as a result of both the angled trench sidewall and the n-bottom assist layer (n-BAL) which allows for the structure to be depleted gradually.

Introduction

Silicon Carbide (SiC) Schottky diodes and power MOSFETs now offer circuit designers a fast-switching alternative to Silicon (Si) PiN diodes and IGBTs within the 600 – 1700 V class. However, despite the low specific on-resistance ($R_{ON,SP}$) of SiC power devices when compared to Si devices, the relationship between $R_{ON,SP}$ and the blocking voltage (V_{BD}) ($R_{ON,SP} \propto V_{BD}^{2.5}$ [1]) limits the use of SiC unipolar devices at higher voltage ratings. As established in Si, superjunction (SJ) devices allows the relationship between $R_{ON,SP}$ and V_{BD} to be almost linearized, reducing the $R_{ON,SP}$ to below the material's unipolar limit. SJ structures thereby reduce on-state losses at higher voltages, whilst maintaining fast switching compared to bipolar devices.

Superjunction devices are achieved by developing highly-doped and perfectly charge balanced n- and p-columns throughout the drift region, as opposed to a single lowly-doped drift region. The requirement for both charge-balanced columns and a high trench aspect ratio (A_{SJ}; the ratio of trench width to trench depth) results in complex process flows. Many of the traditional SJ fabrication techniques developed for Si SJ processing are yet currently not possible in SiC [2]. However, there have been promising developments in SiC SJ fabrication with *Kosugi et al.* [3] demonstrating a 6.8 kV SJ via a trench-refill process, *Baba et al.* demonstrating a 3.3 kV SJ with an epitaxial regrowth and implantation process [4].

Previously, we proposed a 2 kV full-SJ device that could be realised via a trench-etch and tilted implantation [5]. The introduction of a trench sidewall angle of 10°, in reference to the *y*-axis, established a graded charge profile throughout the drift region, resulting in an implantation window that was 20 % wider when compared to the vertical SJ - making device fabrication more likely.

In this paper, both the trench sidewall angle and tilted implantation are introduced into a semi-SJ topology. The impact of the 10° sidewall angle will be analysed via TCAD simulation (Sentaurus) and discussed with the aim of maintaining a $V_{BD} > 2$ kV whilst improving the implantation window.

Device Structure and Simulation Setup

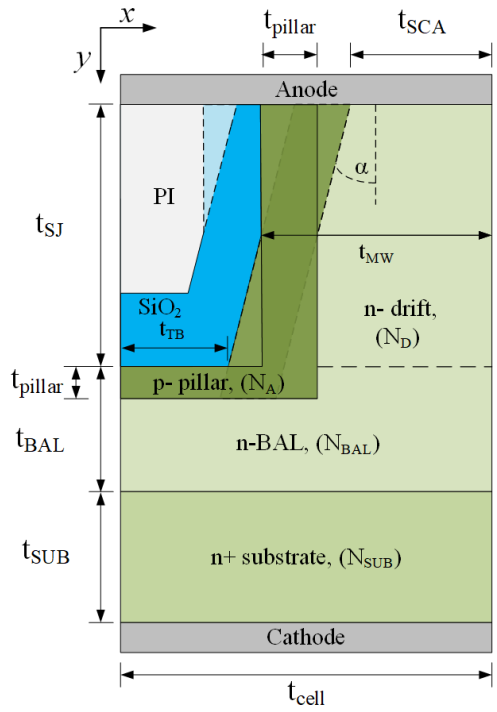

Table I.
Key dimensions and parameters of proposed semi-SJ structure

Symbol	Definition	Value	Units
t_{SJ}	Thickness of drift-region	3.6-9.0	µm
t_{cell}	Cell pitch	4.2	
t_{SCA}	Min. Schottky contact area	1.1	
t_{pillar}	Thickness of p-pillar	0.2	
t_{BAL}	Thickness of BAL	0.0-5.4	
t_{MW}	Mesa-width	2.1	
t_{TB}	Min. Trench Bottom	1.3	
t_{drift}	Total drift region thickness	9.0	
t_{SUB}	Substrate thickness	100	
N_D	Drift region doping	3.5×10^{16}	cm^{-3}
N_{BAL}	Bottom assist layer doping	3.5×10^{16}	
N_A	P-pillar doping	$3.25 - 4.5\times10^{17}$	
N_{SUB}	Substrate doping	1.0×10^{19}	
α	Trench sidewall angle*	0, 10	°
β	Tilted implantation angle*	~30	

* Angles in reference to the *y*-axis

Fig. 1. Half-cell SiC semi-SJ with key dimensions and parameters.

The proposed semi-SJ as can be seen in Fig. 1 and could be developed via a trench-etch and tilted sidewall implantation. The key dimensions and parameters of the proposed structure can be seen in Table 1. The substrate of the structure is 4H-SiC with a doping concentration (N_{SUB}) of 1.0×10^{19} cm^{-3} and a thickness (t_{SUB}) of 100 µm, as if it had been thinned post-processing. The drift-region is the combination of the n-drift (N_D) and the n-BAL (N_{BAL}), both of which have a doping concentration of 3.5×10^{16} cm^{-3}. The structure has a uniform doping concentration throughout to simplify device fabrication. The thickness of both the n-drift and n-BAL (t_{drift}) total 9.0 µm and the thicknesses are split between the t_{BAL}-ratio (= (t_{BAL}/t_{drift})×100). A controllable bevelled-trench profile has been demonstrated in [6]. The p-pillar has a thickness (t_{pillar}) of 200 nm, a doping concentration (N_A), and is assumed to have a box-shape profile. The implantation profile is formed via two Al ions implantations. The first of which is a tilted implantation into both sides of the trench sidewalls, for a given α = 10º a tilted implantation at 30º allows for the Al ions to reach the bottom of the trench. The second implantation is a vertical implant into the trench bottom. The simulated doping concentrations consider the impact of both incomplete ionisation and activation [7], however, the effects of compensation have not been considered. The half-cell mesa width (t_{MW}) is measured at the trench mid-point and has a width of 2.1 µm, with α in reference to the *y*-axis. Pivoting the trench angle about the mid-point allows for charge balance to be maintained with varying degrees of trench sidewall angle (α) for a given t_{BAL}-ratio. A The trench would be passivated with a high-quality SiO_2 layer before being refilled with polyamide (PI). Metal contacts can be formed on the top- and bottom-side of the device. The work-function of the top-side contact is 5.2 eV, similar to that of Ni. The half-cell pitch (t_{cell}) is fixed at 4.2 µm for all devices to ensure comparable current densities. The models utilised within this study have been discussed in our previous work [5].

Simulation Results and Discussion

This paper reports on the TCAD optimisation of semi-SJs with a uniform doping concentration and an angled trench sidewall, as seen in Fig. 1. Firstly, the t_{BAL}-ratio for vertical structures must be identified. As outlined in Fig. 2 (left-left), the N_A was swept for SJ structures with a t_{BAL}-ratio varying between 0 % - 60 %. It should be noted that a t_{BAL}-ratio of 0 % means the structure is a full-SJ. Fig. 2

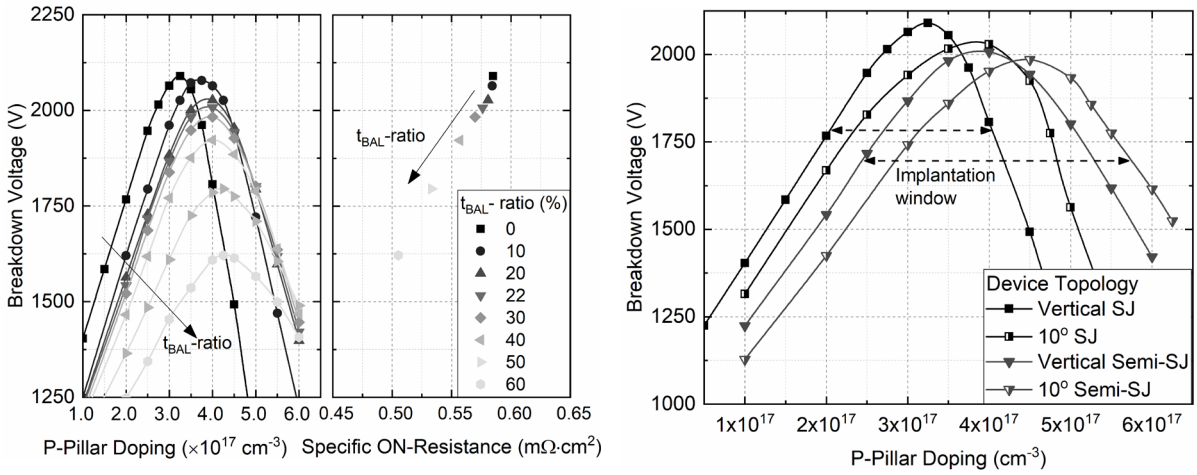

Fig. 2. The impact of t_{BAL} – ratio on the V_{BD} (left-left) and on the $R_{ON,SP}$ (left-right), and the impact of α on the charge balance of both full- and semi-SJs (right).

(left) demonstrates that the full-SJ achieves a V_{BD} of 2090 V and a $R_{ON,SP}$ of 0.59 mΩ·cm^2 – both the highest V_{BD} and $R_{ON,SP}$ in the study. This is because the structure is fully depleted by the alternating SJ pillars and thus achieves the maximum V_{BD}. However, it is worth noting a t_{BAL}-ratio of 10 % also achieves a high V_{BD} of 2080 V and a comparable $R_{ON,SP}$ to the full-SJ, whilst also being easier to fabricate. This shows the true nature of the 2-D field shaping in SJ structures. The thin and highly doped BAL being fully depleted by the p-doping that surrounds the trench bottom. A $V_{BD} > 2$ kV can be maintained up to a t_{BAL}-ratio of 22 %, beyond which a significant reduction in V_{BD} occurs. This is the combined effect of having a shallower SJ region and also a thicker highly doped n-BAL region as t_{BAL} increases. As the value of the t_{BAL} is further increased, the electric field cannot spread into the thicker region, and thus greater proportions of V_{BD} are lost with increasing t_{BAL}.

The $R_{ON,SP}$ of the structures continues to decrease with increasing t_{BAL}-ratio, as can be seen in Fig. 2 (left-right). This is the result of two effects; firstly, the impact of the pinching between the alternating n- and p-pillars is reduced as the t_{SJ} is reduced, and secondly, the additional unbalanced charge within the BAL adds a significant number of carriers to the forward operating state. It must be noted that as the $R_{ON,SP}$ decreases, so does the V_{BD}. As demonstrated in Fig. 2 (left-left), the implantation window (defined as the full-width at 85 % of the peak V_{BD}) is widened from 22-38 % for t_{BAL}-ratios between 10-22 % compared to the vertical full-SJ. The wider implantation window within semi-SJ structures is the result of how the electric field spreads throughout the n-BAL. If the p-pillars are under-doped, a high Q_n condition occurs in the SJ region. This leads to a reduction in V_{BD} as a result of the reduction of the peak electric field at the n-drift/n-BAL interface, which further leads to a reduction in the electric field supported within the n-BAL. Conversely, if the p-pillars are over-doped, a high Q_p condition occurs within the SJ region. This results in a high electric field at the n-drift/n-BAL interface, which in turn allows for a greater electric field to be supported in the n-BAL. This means that semi-SJs offer a greater tolerance to charge imbalance as a result of the peak V_{BD} occurring at high Q_p conditions.

Hereafter, a t_{BAL} of 2.0 µm was used throughout the rest of this study, equating to a t_{BAL}-ratio of 22 %. This structure achieved a $V_{BD} > 2$ kV, a reduced $R_{ON,SP}$ relative to the full-SJ, and an implantation window that was 38 % wider than that of the vertical full-SJ. Having established the t_{BAL}-ratio, a trench sidewall angle (α = 10°) was introduced into the structure. The impact of α was then investigated by sweeping N_A, with the results presented in Fig. 2 (right). It can be seen that the introduction of α increases the implantation window for both the full- and semi-SJs, the mechanisms being described in our previous work [5]. The semi-SJ with a 10° sidewall increases the implantation window by 7 % relative to the vertical semi-SJ and 45 % relative to the vertical full-SJ. Interestingly, the V_{BD} reduction brought about from α is reduced in the semi-SJ when compared to the full-SJ. This is because of the combination of both the graded charge profile and the n-BAL, which aids the modulation of the electric field, even under the presence of charge imbalance. Thus, the semi-SJ with

a graded charge profile offers a significantly wider implantation window and a reduced A_{SJ}, thus increasing its manufacturability.

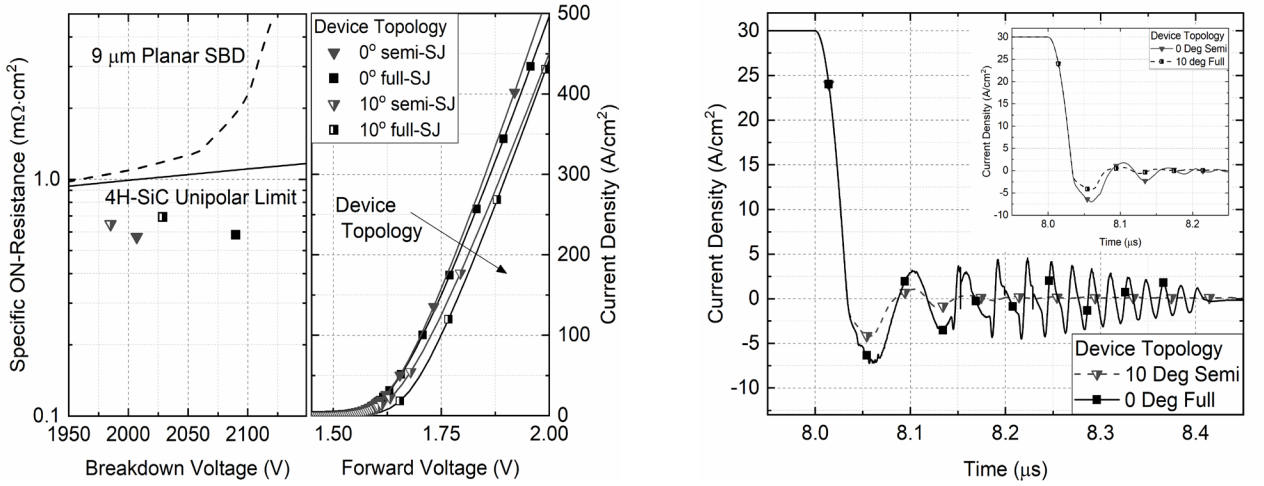

Fig. 3. The proposed structures plotted against the unipolar limit (left-left), the forward state characteristics (left-right), and the switching characteristics (right).

The similar on-state results can be seen in Fig. 3 (left-right) with all devices turning-on around 1.6 V - consistent with the work function of Ni. Fig. 3 (left-right) reveals that the vertical semi-SJ has a comparable $R_{ON,SP}$ to the full-SJ. The impact of $\alpha = 10°$ degrading the device V_{BD} and $R_{ON,SP}$ is reduced when implemented within a semi-SJ topology. The semi-SJ with a 10° sidewall reduces the V_{BD} by 5 % and increases the $R_{ON,SP}$ by 8 %, relative the vertical full-SJ. These characteristics could be recovered by either optimising the n-BAL region and/or by rebalancing the top of the structure.

Finally, it was found that the introduction of the $\alpha = 10°$ allowed for the gradual depletion of the drift region, thus reducing the rapid decrease in dC/dV as the structure is fully depleted. In turn, this allows for smoother switching characteristics as can be seen in Fig. 3 (right) comparing the semi-SJ with a 10° sidewall to the full-SJ. Not only are the effects of ringing suppressed by the gradual depletion of the device, but the peak reverse recovery current is also reduced.

Summary

Simulations have shown that the proposed semi-SJ with a 10° sidewall is a practically realisable solution to SJ design. The structure achieves a wider implantation window and softer switching characteristics whilst only partially degrading the V_{BD} and $R_{ON,SP}$ relative to the full-SJ. The combination of both the graded charge profile with the n-BAL allow for greater tolerance to charge imbalance whilst also allowing the structure to deplete more slowly and thus reducing the dC/dV response, hence producing a softer reverse recovery.

Acknowledgement

The work presented in this paper has been carried out as part of EPSRC project EP/R00448X/1. We gratefully acknowledge this support.

References

[1] B. J. Baliga, *Fundamentals of power semiconductor devices*. Springer Science & Business Media, 2010.

[2] Y. Yonezawa, "Recent Progress in High to Ultra-High-Voltage SiC Power Devices: Development and Application," in *2018 International Power Electronics Conference (IPEC-Niigata 2018-ECCE Asia)*, 2018: IEEE, pp. 3603-3606.

[3] R. Kosugi *et al.*, "Breaking the Theoretical Limit of 6.5 kV-Class 4H-SiC Super-Junction (SJ) MOSFETs by Trench Filling Epitaxial Growth," in *ISPSD*, Shanghai, China, May 19-23 2019.

[4] M. Baba *et al.,* "Ultra-Low Specific on-Resistance Achieved in 3.3 kV-Class SiC Superjunction MOSFET," in *2021 33rd International Symposium on Power Semiconductor Devices and ICs (ISPSD)*, 2021: IEEE, pp. 83-86.

[5] G. Baker *et al.*, "Optimization of 1700-V 4H-SiC Superjunction Schottky Rectifiers With Implanted P-Pillars for Practical Realization," *IEEE Transactions on Electron Devices,* vol. 68, no. 7, pp. 3497 - 3504, 2021.

[6] H.-K. Sung *et al.*, "Vertical and bevel-structured SiC etching techniques incorporating different gas mixture plasmas for various microelectronic applications," *Scientific reports,* vol. 7, no. 1, pp. 1-9, 2017.

[7] J. Pernot *et al.,* "Electrical transport properties of aluminum-implanted 4H–SiC," *Journal of applied physics,* vol. 98, no. 2, p. 023706, 2005.